



ELSEVIER

Nuclear Physics B 527 (1998) 44–60

NUCLEAR  
PHYSICS B

# Seesaw majoron model of neutrino mass and novel signals in Higgs boson production at LEP

Marco A. Díaz<sup>1</sup>, M.A. García-Jareño<sup>2</sup>, Diego A. Restrepo<sup>3</sup>,  
José W.F. Valle<sup>4</sup>

*Departamento de Física Teórica, IFIC-CSIC, Universidad de Valencia, Burjassot, Valencia 46100, Spain*

Received 24 March 1998; accepted 13 May 1998

---

## Abstract

We perform a careful study of the neutral scalar sector of a model which includes a singlet, a doublet, and a triplet scalar field under  $SU(2)$ . This model is motivated by neutrino physics, since it is simply the most general version of the seesaw model of neutrino mass generation through spontaneous violation of lepton number. The neutral Higgs sector contains three  $CP$ -even and one massive  $CP$ -odd Higgs boson  $A$ , in addition to the massless  $CP$ -odd majoron  $J$ . The weakly interacting majoron remains massless if the breaking of lepton number symmetry is purely spontaneous. We show that the massive  $CP$ -odd Higgs boson may invisibly decay to three majorons, as well as to a  $CP$ -even Higgs  $H$  boson plus a majoron. We consider the associated Higgs production  $e^+e^- \rightarrow Z \rightarrow HA$  followed by invisible decays  $A \rightarrow JJJ$  and  $H \rightarrow JJ$  and derive the corresponding limits on masses and coupling that follow from LEP I precision measurements of the invisible  $Z$  width. We also study a novel  $b\bar{b}b\bar{b}\phi_r$  signal predicted by the model, analyze the background and perform a Monte Carlo simulation of the signal in order to illustrate the limits on Higgs boson mass, couplings and branching ratios that follow from that.

© 1998 Elsevier Science B.V.

*PACS:* 14.80.Cp; 13.85.Qk; 11.30.Fs; 12.60.Fr; 14.60.Pq

---

<sup>1</sup> E-mail: mad@flamenco.ific.uv.es

<sup>2</sup> E-mail: miguel@flamenco.ific.uv.es

<sup>3</sup> E-mail: restrepo@flamenco.ific.uv.es

<sup>4</sup> E-mail: valle@flamenco.ific.uv.es

## 1. Introduction

One of main puzzles in particle physics is the origin of mass in general as well as the problem of neutrino mass in particular. In the Standard Model (SM) the spontaneous breaking of the gauge symmetry through the expectation value of a scalar  $SU(2) \otimes U(1)$  doublet is the origin of the masses of the fermions as well as those of the gauge bosons. The main implication for this scenario is the existence of the Higgs boson [1], not yet found [2,3]. Many of the extensions of the Standard Model Higgs sector postulated in order to generate mass for neutrinos are characterized by the spontaneous violation of a global  $U(1)$  lepton number symmetry by an  $SU(2) \otimes U(1)$  singlet vacuum expectation value  $\langle \sigma \rangle$  [4]. These models contain a massless Goldstone boson, called majoron ( $J$ ), which interacts very weakly with normal matter [5]. Although the interactions of the majoron with quarks, leptons, and gauge bosons is naturally very weak, as required also by astrophysics [6], it can have a relatively strong interaction with the Higgs boson [7,8]. It has been noted that the main Higgs boson decay channel is likely to be *invisible*, e.g.

$$H \rightarrow JJ, \quad (1)$$

where  $J$  denotes the majoron field. This feature also appears in variants of the minimal supersymmetric model in which  $R$  parity is broken spontaneously [9]. The phenomenological implications of the invisible  $CP$ -even Higgs boson decays for various collider experiments have been extensively discussed [10–15].

In the seesaw model [16,17] one adds an  $SU(2) \otimes U(1)$  isosinglet right-handed neutrino associated with each generation of isodoublet neutrinos. In addition to the standard lepton number conserving *isodoublet* mass term analogous to those responsible for the charged fermion masses, there is also a Majorana mass term for the right handed neutrinos and left-handed neutrinos. The neutrino mass matrix takes the form

$$\begin{pmatrix} \nu & \nu^c \end{pmatrix}^T \sigma_2 \begin{pmatrix} M_L & D \\ D^T & M_R \end{pmatrix} \begin{pmatrix} \nu \\ \nu^c \end{pmatrix}, \quad (2)$$

where  $\sigma_2$  is the charge conjugation matrix and the entries obey the hierarchy  $M_R \gg D \gg M_L$  [18]. In a model where neutrinos acquire mass only from the spontaneous violation of lepton number the entries  $M_L$  and  $M_R$  arise from vacuum expectation values (VEV) of  $SU(2) \otimes U(1)$  triplet and singlet Higgs scalars  $\Delta$  and  $\sigma$  [19], while the Dirac mass term  $D$  follows from the Standard Model doublet VEV. In this model the light neutrino masses arise from diagonalizing out the heavy right-handed neutrinos and has a contribution from the small triplet VEV.

In this paper we show that, for a wide choice of parameters, the complete version of the seesaw majoron model of neutrino mass containing  $SU(2) \otimes U(1)$  doublet, singlet as well as triplet Higgs multiplets (called **123** model in Ref. [19]) implies that the massive pseudoscalar Higgs boson can also decay invisibly, either directly as

$$A \rightarrow 3J, \quad (3)$$

or indirectly as

$$A \rightarrow HJ \quad \text{with } H \rightarrow JJ \quad (4)$$

when  $m_A > m_H$ . This feature has not been noted in any of the discussions given so far [10,11,13,14], as it is absent in a number of models, for example all the models discussed in [7].

Massive invisibly decaying  $CP$ -odd Higgs bosons may occur in the minimal supersymmetric standard model, where the decay involves a heavy fermion pair,  $A \rightarrow \chi^0 \chi^0$ , with  $\chi^0$  stable due to  $R$ -parity conservation. Similarly, it can also occur in the supersymmetric model with spontaneously broken  $R$ -parity considered in Ref. [9]. In the latter case one could have, e.g.,  $A \rightarrow \chi^0 \chi^0$  or  $A \rightarrow \nu \chi^0$ , with  $\chi^0 \rightarrow \nu J$ , where  $J$  denotes the majoron. However, all these decays require a kinematical condition  $m_A > 2m_{\chi^0}$  or  $m_A > m_{\chi^0}$  which is avoided here due to the majoron being massless.

We carefully study the scalar potential of the model and derive from it the relevant  $CP$ -even as well as  $CP$ -odd Higgs boson mass matrices. In the next section, we discuss the parameterization of Higgs bosons couplings relevant for their production at LEP, both for the  $ZH$  as well as  $AH$  production channels. Next we use these theoretical results in order to derive restrictions on the relevant Higgs boson parameters from the precision measurements of the invisible width of the  $Z$  boson at LEP I. The associated production  $e^+e^- \rightarrow HA$  with  $A \rightarrow HJ$  and  $H \rightarrow b\bar{b}$  also leads to a novel  $b\bar{b}b\bar{b}\cancel{p}_T$  signal topology that could be detectable at LEP II. We have performed a detailed analysis of the background and carried out a Monte Carlo simulation of the signal in order to illustrate the limits on Higgs boson mass, couplings and branching ratios that follow from four-jet + missing momentum signal topology.

## 2. The scalar potential

The model we consider here is the one proposed in Ref. [19] as a generalization of the triplet [20] and singlet [5] majoron models. The Higgs sector of the model contains the usual  $SU(2)$  Higgs complex doublet  $\phi$  of the SM, with lepton number  $L = 0$ , and an  $SU(2)$  complex triplet  $\Delta$ , with lepton number  $L = -2$ ,

$$\Delta = \begin{bmatrix} \Delta^0 & \Delta^+/\sqrt{2} \\ \Delta^+/\sqrt{2} & \Delta^{++} \end{bmatrix}, \quad \phi = \begin{bmatrix} \phi^0 \\ \phi^- \end{bmatrix}, \quad (5)$$

where we have used the  $2 \times 2$  matrix notation for the Higgs triplet given in Ref. [21]. The Higgs sector is completed with a complex  $SU(2) \otimes U(1)$  singlet scalar, denoted  $\sigma$ , carrying lepton number  $L = 2$ .

The full scalar potential is given by [22]

$$V(\phi, \Delta, \sigma) = \mu_2^2 \phi^\dagger \phi + \mu_3^2 \text{tr}(\Delta^\dagger \Delta) + \lambda_1 (\phi^\dagger \phi)^2 + \lambda_2 [\text{tr}(\Delta^\dagger \Delta)]^2 \\ + \lambda_3 \phi^\dagger \phi \text{tr}(\Delta^\dagger \Delta) + \lambda_4 \text{tr}(\Delta^\dagger \Delta \Delta^\dagger \Delta) + \lambda_5 (\phi^\dagger \Delta^\dagger \Delta \phi)$$

$$\begin{aligned}
& +\mu_1^2\sigma^\dagger\sigma + \beta_1(\sigma^\dagger\sigma)^2 + \beta_2(\phi^\dagger\phi)(\sigma^\dagger\sigma) \\
& +\beta_3\text{tr}(\Delta^\dagger\Delta)\sigma^\dagger\sigma - \kappa(\phi^T\Delta\phi\sigma + \text{h.c.})
\end{aligned} \tag{6}$$

where  $\mu_i$ ,  $i = 1, 2, 3$ , are mass parameters, and  $\lambda_i$ ,  $i = 1, \dots, 5$ ,  $\beta_i$ ,  $i = 1, 2, 3$ , and  $\kappa$  are dimensional-less couplings. The first two lines in Eq. (6) correspond to the Gelmini–Roncadelli model [20], and the last two lines are new terms involving the scalar  $\sigma$ . The term in  $\kappa$  has been introduced in Ref. [19] and plays an important role in our present discussion.

The singlet  $\sigma$ , as well as the neutral components of the fields  $\phi$  and  $\Delta$ , acquire vacuum expectation values  $v_1$ ,  $v_2$ , and  $v_3$  respectively. According to this, we shift the fields in the following way:

$$\begin{aligned}
\sigma &= \frac{v_1}{\sqrt{2}} + \frac{R_1 + iI_1}{\sqrt{2}}, \\
\phi^0 &= \frac{v_2}{\sqrt{2}} + \frac{R_2 + iI_2}{\sqrt{2}}, \\
\Delta^0 &= \frac{v_3}{\sqrt{2}} + \frac{R_3 + iI_3}{\sqrt{2}}.
\end{aligned} \tag{7}$$

We assume that the three vacuum expectation values are real. The scalar potential contains the following linear terms:

$$V_{\text{linear}} = t_1 R_1 + t_2 R_2 + t_3 R_3, \tag{8}$$

where

$$\begin{aligned}
t_1 &= v_1(\mu_1^2 + \beta_1 v_1^2 + \frac{1}{2}\beta_2 v_2^2 + \frac{1}{2}\beta_3 v_3^2) - \frac{1}{2}\kappa v_2^2 v_3, \\
t_2 &= v_2(\mu_2^2 + \lambda_1 v_2^2 + \frac{1}{2}\lambda_3 v_3^2 + \frac{1}{2}\lambda_5 v_3^2 + \frac{1}{2}\beta_2 v_1^2 - \kappa v_1 v_3), \\
t_3 &= v_3(\mu_3^2 + \lambda_2 v_3^2 + \frac{1}{2}\lambda_3 v_2^2 + \lambda_4 v_3^2 + \frac{1}{2}\lambda_5 v_2^2 + \frac{1}{2}\beta_3 v_1^2) - \frac{1}{2}\kappa v_1 v_2^2.
\end{aligned} \tag{9}$$

The conditions for a extreme of the potential are  $t_i = 0$ ,  $i = 1, 2, 3$ . Therefore, the  $t_i = 0$  vanish at the minima of the potential. We will verify explicitly below that, for many choices of its parameters, the potential has indeed minima for non-zero values of  $v_1$ ,  $v_2$  and  $v_3$ .

### 3. Neutral Higgs mass matrices

Taking into account the fact that this model contains one doubly charged and one singly charged scalar boson, in addition to the two charged unphysical  $SU(2) \otimes U(1)$  Goldstone modes (longitudinal  $W$ ), it follows that the neutral Higgs sector of this model is composed by six real fields. Due to  $CP$  invariance they split into two unmixed sectors of three  $CP$ -even and three  $CP$ -odd fields. Their mass matrices are contained in the quadratic scalar potential which includes

$$V_{\text{quadratic}} = \frac{1}{2} [R_1, R_2, R_3] \mathbf{M}_R^2 \begin{bmatrix} R_1 \\ R_2 \\ R_3 \end{bmatrix} + \frac{1}{2} [I_1, I_2, I_3] \mathbf{M}_I^2 \begin{bmatrix} I_1 \\ I_2 \\ I_3 \end{bmatrix} + \dots \quad (10)$$

The  $CP$ -even Higgs mass matrix, which is in agreement with Ref. [22], is given by

$$\mathbf{M}_R^2 = \begin{bmatrix} 2\beta_1 v_1^2 + \frac{1}{2} \kappa v_2^2 \frac{v_3}{v_1} + \frac{t_1}{v_1} & \beta_2 v_1 v_2 - \kappa v_2 v_3 & \beta_3 v_1 v_3 - \frac{1}{2} \kappa v_2^2 \\ \beta_2 v_1 v_2 - \kappa v_2 v_3 & 2\lambda_1 v_2^2 + \frac{t_2}{v_2} & (\lambda_3 + \lambda_5) v_2 v_3 - \kappa v_1 v_2 \\ \beta_3 v_1 v_3 - \frac{1}{2} \kappa v_2^2 & (\lambda_3 + \lambda_5) v_2 v_3 - \kappa v_1 v_2 & 2(\lambda_2 + \lambda_4) v_3^2 + \frac{1}{2} \kappa v_2^2 \frac{v_1}{v_3} + \frac{t_3}{v_3} \end{bmatrix} \quad (11)$$

where it is safe to take  $t_i = 0$ ,  $i = 1, 2, 3$ , unless  $v_1 = 0$  or  $v_3 = 0$  in which case the expression of the corresponding extremization condition (“tadpole equation”) in Eq. (9) must be replaced in the mass matrix  $\mathbf{M}_R^2$ . The physical  $CP$ -even mass eigenstates  $H_i$ ,  $i = 1, 2, 3$ , are related to the corresponding weak eigenstates  $R_i$  as

$$\begin{bmatrix} H_1 \\ H_2 \\ H_3 \end{bmatrix} = O_R \begin{bmatrix} R_1 \\ R_2 \\ R_3 \end{bmatrix}, \quad (12)$$

where the  $3 \times 3$  matrix  $O_R$  is the matrix which diagonalizes the  $CP$ -even mass matrix such that

$$O_R \mathbf{M}_R^2 O_R^T = \text{diag}(m_{H_1}^2, m_{H_2}^2, m_{H_3}^2) \quad (13)$$

and where by definition we take  $m_{H_1} \leq m_{H_2} \leq m_{H_3}$ .

The  $CP$ -odd Higgs mass matrix  $\mathbf{M}_I^2$  is given by [19]

$$\mathbf{M}_I^2 = \begin{bmatrix} \frac{1}{2} \kappa v_2^2 \frac{v_3}{v_1} + \frac{t_1}{v_1} & \kappa v_2 v_3 & \frac{1}{2} \kappa v_2^2 \\ \kappa v_2 v_3 & 2\kappa v_1 v_3 + \frac{t_2}{v_2} & \kappa v_1 v_2 \\ \frac{1}{2} \kappa v_2^2 & \kappa v_1 v_2 & \frac{1}{2} \kappa v_2^2 \frac{v_1}{v_3} + \frac{t_3}{v_3} \end{bmatrix}. \quad (14)$$

If  $v_1 \neq 0$  and  $v_3 \neq 0$  we can safely set the tadpoles equal to zero in Eq. (14), in whose case we can see that the matrix  $\mathbf{M}_I^2$  has two zero eigenvalues. One of them is the unphysical Goldstone boson and the other is the physical Majoron. The physical  $CP$ -odd mass eigenstates  $A_i$ ,  $i = 1, 2, 3$ , are related to the corresponding weak eigenstates  $I_i$  as

$$\begin{bmatrix} A_1 \\ A_2 \\ A_3 \end{bmatrix} \equiv \begin{bmatrix} J \\ G \\ A \end{bmatrix} = O_I \begin{bmatrix} I_1 \\ I_2 \\ I_3 \end{bmatrix}, \quad (15)$$

where the  $3 \times 3$  matrix  $O_I$  is the matrix which diagonalizes the  $CP$ -odd mass matrix such that

$$O_I \mathbf{M}_I^2 O_I^T = \text{diag}(0, 0, m_A^2) \quad (16)$$

and the  $CP$ -odd Higgs mass is given by

$$m_A^2 = \frac{1}{2} \kappa \frac{v_2^2 v_1^2 + v_2^2 v_3^2 + 4v_3^2 v_1^2}{v_3 v_1}. \quad (17)$$

Note that  $m_A \rightarrow 0$  as  $\kappa \rightarrow 0$ . The diagonalization matrix  $O_I$  can be found analytically

$$O_I = \begin{bmatrix} cv_1 V^2 & -2cv_2 v_3^2 & -cv_2^2 v_3 \\ 0 & v_2/V & -2v_3/V \\ bv_2/2v_1 & b & bv_2/2v_3 \end{bmatrix}, \quad (18)$$

where  $V$ ,  $c$ , and  $b$  are the normalization constants for the eigenvectors  $G$ ,  $J$ ,  $A$  respectively. They are given by

$$\begin{aligned} V^2 &= v_2^2 + 4v_3^2, \\ c^{-2} &= v_1^2 V^4 + 4v_2^2 v_3^4 + v_2^4 v_3^2, \\ b^2 &= \frac{4v_1^2 v_3^2}{v_2^2 v_1^2 + v_2^2 v_3^2 + 4v_3^2 v_1^2}. \end{aligned} \quad (19)$$

We now briefly discuss three special cases, motivated by the cases when tadpoles cannot be trivially set to zero in the scalar mass matrices  $\mathbf{M}_R^2$  and  $\mathbf{M}_I^2$ .

(i)  $v_1 = 0$ ,  $v_3 = 0$ .

In this case there is no breaking of lepton number, as in the Standard Model and, as a result there is no massless Majoron. The unphysical Goldstone boson is purely doublet. One of the  $CP$ -even Higgs bosons is also pure doublet with a mass  $m_H^2 = 2\lambda_1 v_2^2$ . The remaining two  $CP$ -even Higgs bosons are massive and are a mixture of singlet and triplet. There are also two massive  $CP$ -odd Higgs bosons and they are degenerate with the  $CP$ -even Higgs bosons.

(ii)  $v_1 \neq 0$ ,  $v_3 = 0$ .

In this case the third minimization equation forces to have  $\kappa = 0$ . There is a Majoron with  $m_J = 0$  which is purely singlet, as in the simplest **12** model considered in Ref. [19], and the unphysical Goldstone boson is purely doublet. The real and imaginary parts of the neutral component of the triplet field are degenerate and form a complex field with mass  $m_{\Delta^0}^2 = \mu_3^2 + \frac{1}{2}(\lambda_3 + \lambda_5)v_2^2 + \frac{1}{2}\beta_3 v_1^2$ . There are two additional massive  $CP$ -even Higgs bosons, mixture of singlet and doublet.

(iii)  $v_1 = 0$ ,  $v_3 \neq 0$ .

In this case the first tadpole equation forces to have  $\kappa = 0$ . There is a Majoron with  $m_J = 0$  which has zero component along the singlet, and is therefore experimentally ruled out by the LEP data. Here the situation is analogous to the simplest **23** model of Ref. [19] and it is for this reason that the presence of the singlet field  $\sigma$  with non-zero VEV is mandatory.

Thus we conclude that the situation of interest for us is the general one in which all three VEVs  $v_1$ ,  $v_2$  and  $v_3$  take on non-zero values. In our numerical calculations reported

in Section 5 we must take into account an important astrophysical constraint on these VEVs that follows from stellar cooling by majoron emission which severely restricts the majoron electron coupling to be less than about  $10^{-12}$  or so. This is discussed in detail in Section 5.

#### 4. Higgs boson production and decays

In this section we derive the couplings relevant for Higgs boson production at  $e^+e^-$  colliders and for their invisible decays. The two production mechanisms we consider are the emission of a  $CP$ -even Higgs  $H$  by a  $Z$ -boson, and the associated production consisting of a  $Z$ -boson decaying into a  $CP$ -even Higgs  $H$  and a  $CP$ -odd Higgs  $A$ . In order to derive the couplings  $ZZH$  and  $ZHA$ , we need the kinetic part of the scalar Lagrangian contained in

$$\mathcal{L}_{\text{scalar}} = (\mathcal{D}_\mu \phi)^\dagger \mathcal{D}^\mu \phi + \text{tr} [(\mathcal{D}_\mu \Delta)^\dagger \mathcal{D}^\mu \Delta] + \partial_\mu \sigma^\dagger \partial^\mu \sigma - V(\phi, \Delta, \sigma), \quad (20)$$

where the covariant derivative is defined by

$$\mathcal{D} = \partial^\mu + ig\mathbf{T} \cdot \mathbf{W}^\mu + \frac{i}{2}g'YV^\mu \quad (21)$$

and  $g$  and  $g'$  are the gauge couplings corresponding to the  $SU(2)$  and  $U(1)$  groups respectively. On the scalars fields, the generators act as follows:

$$\begin{aligned} \mathbf{T}\phi &= \frac{1}{2}\boldsymbol{\tau}\phi, & \mathbf{T}\Delta &= -\frac{1}{2}\boldsymbol{\tau}\Delta - \frac{1}{2}\Delta\boldsymbol{\tau}^*, \\ Y\phi &= -1\phi, & Y\Delta &= 2\Delta, \end{aligned} \quad (22)$$

and with these definitions we have  $T_3\phi^0 = \frac{1}{2}\phi^0$  and  $T_3\Delta^0 = -1\Delta^0$ .

The Higgs singlet does not contribute to the gauge boson masses, therefore, they depend only on  $v_2$  and  $v_3$  and are given by [18]

$$m_Z^2 = \frac{g^2}{4\cos^2\theta_W}(v_2^2 + 4v_3^2), \quad m_W^2 = \frac{g^2}{4}(v_2^2 + 2v_3^2) \quad (23)$$

and from the measurement of the  $\rho$  parameter one has a restriction on  $v_3$ , namely [23]

$$\rho = 1 + \frac{2v_3^2}{v_2^2 + 2v_3^2} = 1.001 \pm 0.002. \quad (24)$$

which implies in practice that  $v_3 \leq 8$  GeV.

We now calculate the relevant couplings for the production of Higgs bosons at  $e^+e^-$  colliders. Using Eq. (20), we determined the  $HAZ$  couplings to be

$$\begin{aligned} \mathcal{L}_{HAZ} &= \frac{g}{2c_W} Z^\mu \left[ R_2 \overset{\leftrightarrow}{\partial}^\mu I_2 - 2R_3 \overset{\leftrightarrow}{\partial}^\mu I_3 \right] \\ &= \frac{g}{2c_W} Z^\mu \left[ O_{32}^I O_{a2}^R - 2O_{33}^I O_{a3}^R \right] H_a \overset{\leftrightarrow}{\partial}^\mu A, \end{aligned} \quad (25)$$

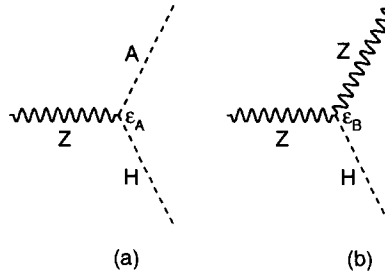


Fig. 1. Feynman rules relevant to Bjorken and associated Higgs production.

where  $c_W \equiv \cos \theta_W$  and  $H_a$  is any of the three  $CP$ -even neutral Higgs bosons. The quantity defined by

$$\epsilon_A = O_{32}^I O_{12}^R - 2O_{33}^I O_{13}^R \quad (26)$$

essentially represents the strength of the coupling  $H_1AZ$  [see the second squared parenthesis in Eq. (25)].

From Eq. (20) we find that the  $HZZ$  coupling is

$$\mathcal{L}_{HZZ} = \frac{g}{4c_W^2} m_Z Z^\mu Z_\mu \left[ \frac{v_2}{V} O_{a2}^R + \frac{4v_3}{V} O_{a3}^R \right] H_a, \quad (27)$$

and again we define the following quantity:

$$\epsilon_B = \frac{v_2}{V} O_{12}^R + \frac{4v_3}{V} O_{13}^R, \quad (28)$$

as a measure of the strength of the  $H_1ZZ$  coupling. Therefore, the Bjorken production mechanism (Fig. 1a) and the associated production mechanism (Fig. 1b) are determined by the parameters  $\epsilon_A$  and  $\epsilon_B$  respectively.

We now turn to the couplings relevant for the invisible decay of the Higgs bosons  $H_1$  and  $A$ . We need to find first the trilinear couplings  $HJJ$ ,  $H AJ$ , and  $HAA$ , thus we start with the cubic part of the scalar potential which involve one (unrotated)  $CP$ -even Higgs field  $R_i$  and two (unrotated)  $CP$ -odd Higgs fields  $I_j$ . This part of the potential is given by

$$\begin{aligned} V_{RII} = & \lambda_1 v_2 I_2^2 R_2 + (\lambda_2 + \lambda_4) v_3 I_3^2 R_3 + \frac{1}{2} (\lambda_3 + \lambda_5) (v_2 I_3^2 R_2 + v_3 I_2^2 R_3) \\ & + \beta_1 v_1 I_1^2 R_1 + \frac{1}{2} \beta_2 (v_2 I_1^2 R_2 + v_1 I_2^2 R_1) + \frac{1}{2} \beta_3 (v_1 I_3^2 R_1 + v_3 I_1^2 R_3) \\ & + \kappa [v_1 (\frac{1}{2} I_2^2 R_3 + I_2 I_3 R_2) + v_3 (\frac{1}{2} I_2^2 R_1 + I_1 I_2 R_2) \\ & + v_2 (I_1 I_2 R_3 + I_3 I_1 R_2 + I_2 I_3 R_1)]. \end{aligned} \quad (29)$$

Making the substitution  $I_i I_j \rightarrow O_{1i}^I O_{1j}^I J^2$  in Eq. (29), we find the coupling  $H_a J J$  in terms of the mass  $m_{H_a}$  and the rotation matrices  $O^R$  and  $O^I$

$$\begin{aligned}
V_{HJJ} &= \frac{1}{2} \left[ \frac{O_{12}^{\prime 2}}{v_2} (M_R^2)_{1a} + \frac{O_{13}^{\prime 2}}{v_3} (M_R^2)_{2a} + \frac{O_{11}^{\prime 2}}{v_1} (M_R^2)_{3a} \right] R_a J^2 \\
&= \frac{1}{2} \left[ \frac{O_{12}^{\prime 2}}{v_2} (O^R)_{2a}^T + \frac{O_{13}^{\prime 2}}{v_3} (O^R)_{3a}^T + \frac{O_{11}^{\prime 2}}{v_1} (O^R)_{1a}^T \right] m_{Ha}^2 H_a J^2, \quad (30)
\end{aligned}$$

where Eq. (13) has been used.

In a similar way, the terms in the Lagrangian relevant for the vertices  $HAJ$  and  $HAA$  can be found from Eq. (29) making the following substitutions:

$$\begin{aligned}
V_{HAJ} &= V_{RII} (I_i I_j \rightarrow [O_{3i}^{\prime} O_{1j}^{\prime} + O_{1i}^{\prime} O_{3j}^{\prime}] AJ), \\
V_{HAA} &= V_{RII} (I_i I_j \rightarrow O_{3i}^{\prime} O_{3j}^{\prime} A^2). \quad (31)
\end{aligned}$$

These terms are not explicitly displayed.

Finally we turn to the quartic coupling responsible for the invisible decay  $A \rightarrow 3J$ . The relevant piece of the quartic scalar potential is

$$\begin{aligned}
V_J^4 &= \frac{1}{4} [\lambda_1 I_2^4 + (\lambda_2 + \lambda_4) I_3^4 + (\lambda_3 + \lambda_5) I_2^2 I_3^2 + \beta_1 I_1^4 + \beta_2 I_2^2 I_1^2 \\
&\quad + \beta_3 I_3^2 I_1^2 - 2\kappa I_1 I_2^2 I_3] \quad (32)
\end{aligned}$$

and after making the substitution

$$I_i I_j I_k^2 \rightarrow (O_{3i}^{\prime} O_{1j}^{\prime} O_{1k}^{\prime 2} + O_{1i}^{\prime} O_{3j}^{\prime} O_{1k}^{\prime 2} + 2O_{1i}^{\prime} O_{1j}^{\prime} O_{3k}^{\prime} O_{1k}^{\prime}) AJ^3, \quad (33)$$

we find the term  $AJ^3$  in the scalar potential:

$$\begin{aligned}
V_{AJ^3} &= \left[ \lambda_1 O_{12}^{\prime 3} O_{32}^{\prime} + (\lambda_2 + \lambda_4) O_{13}^{\prime 3} O_{33}^{\prime} + \frac{1}{2} (\lambda_3 + \lambda_5) O_{12}^{\prime} O_{13}^{\prime} (O_{32}^{\prime} O_{13}^{\prime} + O_{33}^{\prime} O_{12}^{\prime}) \right. \\
&\quad + \beta_1 O_{11}^{\prime 3} O_{31}^{\prime} + \frac{1}{2} \beta_2 O_{11}^{\prime} O_{12}^{\prime} (O_{31}^{\prime} O_{12}^{\prime} + O_{32}^{\prime} O_{11}^{\prime}) \\
&\quad \left. + \frac{1}{2} \beta_3 O_{11}^{\prime} O_{13}^{\prime} (O_{31}^{\prime} O_{13}^{\prime} + O_{33}^{\prime} O_{11}^{\prime}) - \kappa (O_{31}^{\prime} O_{13}^{\prime} O_{12}^{\prime 2} + O_{11}^{\prime} O_{12}^{\prime} O_{13}^{\prime} O_{32}^{\prime}) \right] AJ^3, \quad (34)
\end{aligned}$$

which complete all the relevant information necessary to calculate the production and invisible decay of the Higgs bosons.

## 5. Numerical expectations of the model

In this section we describe the expectations of our Model for the various Higgs boson masses and couplings relevant for our discussion. In order to do this we numerically diagonalize the mass matrix in Eq. (11) and impose the minimization conditions  $t_i = 0$ ,  $i = 1, 2, 3$ , where the tadpoles are in Eq. (9), and check the positivity of the three  $CP$ -even and  $CP$ -odd eigenvalues. As seen explicitly, these matrices are determined in terms of the nine dimensionless coupling constants and the three VEVs characterising the Higgs potential, as the three mass parameters  $\mu_i$  have all been eliminated. Note,

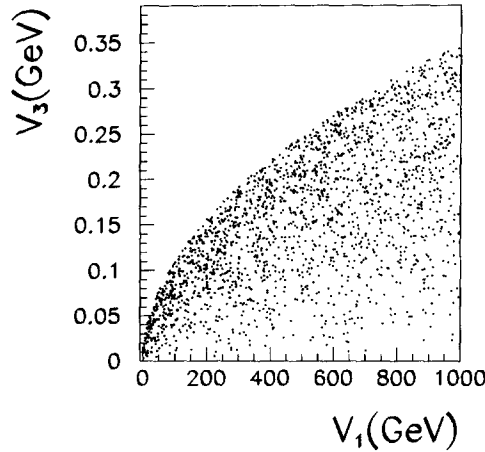


Fig. 2. Allowed region in  $v_1$ - $v_3$  space obtained when the parameters are varied as described in the text.

however that there is a restriction that arises from the  $W$  mass constraint that relates  $v_2$  and  $v_3$  through Eq. (23) that can be written as

$$\sqrt{v_2^2 + 2v_3^2} \simeq 246 \text{ GeV} \quad (35)$$

Moreover,  $v_3$  must be smaller than about 8 GeV in order to obey the experimental value of the  $\rho$  parameter defined in Eq. (24).

A more stringent constraint on  $v_3$  follows from astrophysics, due to the stellar cooling argument, already mentioned. Indeed, if produced in a stellar environment via the Compton-like process  $\gamma + e \rightarrow J + e$ , the majoron would escape leading to excessive energy loss [6]. In order to suppress this one must severely restrict the coupling of the Majoron to the electrons. Such coupling arises from the projection of the majoron  $J$  onto the doublet, leading to

$$|\langle J | \phi \rangle| = \frac{2|v_2|v_3^2}{\sqrt{v_1^2(v_2^2 + 4v_3^2)^2 + 4v_2^2v_3^4 + v_2^4v_3^2}} \lesssim 10^{-6}. \quad (36)$$

In order to have an idea of the parameter ranges involved we have randomly varied over the parameters  $0 < \lambda_i < 4$ ,  $0 < \beta_i < 4$ , (in order to guarantee a perturbative regime) and the three  $v_i$  subject to the above restrictions, with the lepton number violating  $v_1$  varied in the range  $0 < v_1 < 1000$  GeV. The resulting  $v_1$ - $v_3$  region allowed by the model is seen in Fig. 2. The shape of the region can be understood easily from Eq. (36) noting that, since the lepton number violating VEV  $v_3$  is small and  $v_2$  is almost fixed by the  $W$  mass constraint, then the boundary of the allowed region satisfies  $v_3 \sim \sqrt{v_1}$ .

The lowest-lying Higgs boson masses in our model may be similarly determined after imposing the above restrictions. For example, it is instructive to display the results as a function of the parameter  $\kappa$  characterising the Higgs potential. The corresponding plots are shown in Figs. 3a,b. In Fig. 3a we plot the correlation between the massive pseudoscalar mass and the parameter  $\kappa$ , for different values of  $v_1$ . Each curve corresponds

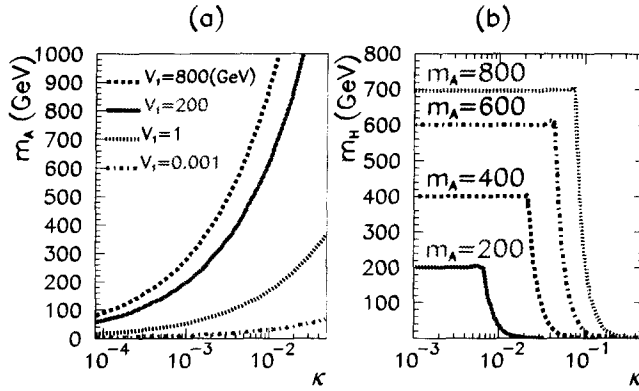


Fig. 3. Lowest-lying Higgs boson masses allowed in our model when the parameters are varied as described in the text.

to the boundary of a scatter plot with the solutions concentrated above it. Its shape can be understood from Eq. (17) and Eq. (36) where we find  $m_A \sim \sqrt{\kappa}$ . In order to have  $m_A$  below a certain value one requires an upper bound on  $\kappa$ , which tightens with larger  $v_1$ . From Fig. 3b, we can see that, as a consequence of the smallness of  $v_3$ ,  $m_{H_1} < m_A$ , except for a narrow window in which  $m_{H_1} \gtrsim m_A$ . This region is so small that it cannot even be appreciated in the figure, since it is smaller than the thickness of the line itself. In such a small region the decay  $H_1 \rightarrow AJ$  would be allowed, while the decay  $H_1 \rightarrow AA$  is forbidden by phase space. This can be contrasted with the MSSM where the decay  $h \rightarrow AA$  is allowed, though in a very small region in parameter space [24]. When  $\kappa$  is small  $H_1$  is mostly triplet and almost degenerate with  $A$  and this corresponds to the horizontal lines in Fig. 3b. For larger  $\kappa$  the component of  $H_1$  along the triplet decreases and  $H_1$  becomes lighter than  $A$ , as seen in Fig. 3b.

We have verified explicitly that in our model the invisible branching ratios of  $H_1$  and  $A$  given by<sup>5</sup>

$$\begin{aligned} B_{\text{inv}} &= \text{BR}(H_1 \rightarrow JJ) + \text{BR}(H_1 \rightarrow JA)\text{BR}(A \rightarrow JJJ), \\ A_{\text{inv}} &= \text{BR}(A \rightarrow JJJ) + \text{BR}(A \rightarrow JH_1)\text{BR}(H_1 \rightarrow JJ), \end{aligned} \quad (37)$$

and their product  $B_{\text{inv}} A_{\text{inv}}$ , which will be needed in the next section, can be large and even 100% over large regions of the parameter space. This can be seen in Fig. 4 where we are considering only points in parameter space where  $B_{\text{inv}} A_{\text{inv}} > 0.9$ . We also have verified that  $\epsilon_A^2$  can vary over all its range for all possible values of the invisible branching ratios. Thus, one may obtain plots similar to Fig. 4a for other possible values of the product  $B_{\text{inv}} A_{\text{inv}}$ . The solutions where  $\epsilon_A^2$  is larger than the label associated to a particular curve are concentrated in the region between the curve and the main diagonal. The points corresponding to  $\epsilon_A^2 > 0.4$  are so close to the main diagonal that the width of the region cannot be seen with the naked eye. An alternative way to display this

<sup>5</sup> We have neglected the invisible decay  $A \rightarrow \nu\nu$  relative to  $A \rightarrow 3J$ , which is expected for reasonable choices for the quartic parameters in the scalar Higgs potential and for the lepton Yukawa couplings.

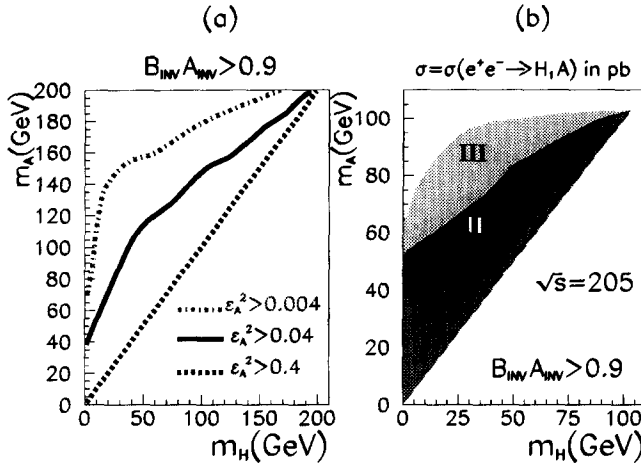


Fig. 4. Lowest-lying Higgs boson masses versus effective coupling strength parameter (a) and associated production cross section (b).

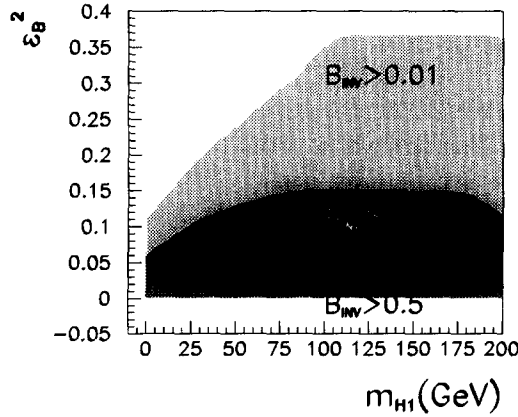


Fig. 5. Bjorken production effective strength parameter versus  $m_{H_1}$  for different ranges of the parameter  $B_{inv}$ .

information is in terms of the associated production cross section which we choose to calculate at  $\sqrt{s} = 205$  GeV. This is shown in Fig. 4b. In this figure the diagonal line corresponds to the maximum cross section  $\sigma_{max} \approx 0.5$  pb, while region I corresponds to points where the cross section lies between 0.1 pb and 0.5 pb. For region II we have  $0.1 > \sigma \geq 0.01$  pb and for region III,  $0.01 > \sigma \geq 0.001$  pb. Note that there are no points with  $m_{H_1} > m_A$  except very near the line  $m_A = m_{H_1}$ . For completeness we also present in Fig. 5 the results for the Bjorken production. This plot displays the effective coupling strength parameter  $\epsilon_B^2$  versus  $m_{H_1}$  for different ranges of the invisible branching ratio  $B_{inv}$ . Note that  $B_{inv}$  is large only when the coupling of the lightest  $CP$ -even Higgs onto the doublet Higgs boson,  $O_{12}^R$ . Should it be small the corresponding value of  $\epsilon_B \approx O_{12}^R$  which determines the Bjorken cross section is also small. This correlation

Table 1

Final signals arising from associated production (left column) as well Bjorken production (right column)

Associated production	Bjorken production
$b\bar{b}b\bar{b}$	$b\bar{b}\cancel{p}_T$
$b\bar{b}\cancel{p}_T$	$b\bar{b}l^+l^-$
$b\bar{b}b\bar{b}\cancel{p}_T$	$b\bar{b}q\bar{q}$
$\cancel{p}_T$	$l^+l^-\cancel{p}_T$
	$l^+l^-\cancel{p}_T$
	$\cancel{p}_T$

can easily be seen from Fig. 5. As a result, if the Higgs is produced via the Bjorken process it is likely to decay visibly, as in the SM.

## 6. Model-independent analysis

In this section we perform a model independent study of the limits that can be set based on Higgs boson production in  $e^+e^-$  colliders and its subsequent decays, focusing on LEP.

Consider the massive pseudoscalar  $A$  and the lightest  $CP$ -even scalar  $H_1$ . If  $m_A > m_{H_1}$  then  $A$  may decay in the standard way to  $b\bar{b}$ , or to  $b\bar{b} + \cancel{p}_T$  via  $A \rightarrow H_1 J$  with  $H_1 \rightarrow b\bar{b}$ , or invisibly into three majorons. From unitarity it follows that only two of these three branching ratios are independent. In addition, the lightest scalar boson  $H_1$  can decay either to  $b\bar{b}$  or invisibly to two majorons and only one of the two branching ratios is independent. Similarly, if  $m_{H_1} > m_A$  we have in total three independent branching ratios. Thus, in order to make a model independent analysis, we need seven parameters to describe the implications of the production of Higgs bosons at the  $Z$  peak: two masses  $m_A$  and  $m_{H_1}$ , the two parameters  $\epsilon_A$  and  $\epsilon_B$  which determine the Bjorken and associated production cross sections and finally, three independent branching ratios (two for the heavier Higgs boson and one for the lightest). Table 1 shows the signatures expected in the model for the cases of Bjorken and Associated production.

In order to have an idea one may compare the above seven parameters with those needed in the simpler models considered before. In the majoron-less model in Ref. [25] only five parameters would be relevant, as there is a unitarity relation  $\epsilon_B^2 + \epsilon_A^2 = 1$  which does not hold in the present case because the admixture of the singlet Higgs bosons reduces the  $H$  and  $A$  couplings to the  $Z$ . The present model has the additional  $A \rightarrow HJ$  branching ratio. Moreover in Ref. [25] the  $A$  must decay either visibly (mainly to  $b\bar{b}$ ) or invisibly to neutrinos. On the other hand in the majoron model considered in Ref. [14] there are also five parameters:  $m_A$ ,  $m_H$ ,  $\epsilon_B$ ,  $\epsilon_A$  and finally, the visible  $H$  decay branching ratio is an arbitrary parameter. Note that the  $A$  must decay visibly (to  $b\bar{b}$  mainly) but there is no unitarity relation for the  $\epsilon$ 's due to the admixture of the singlet Higgs bosons.

It is outside the scope of our present paper to perform an exhaustive study of re-

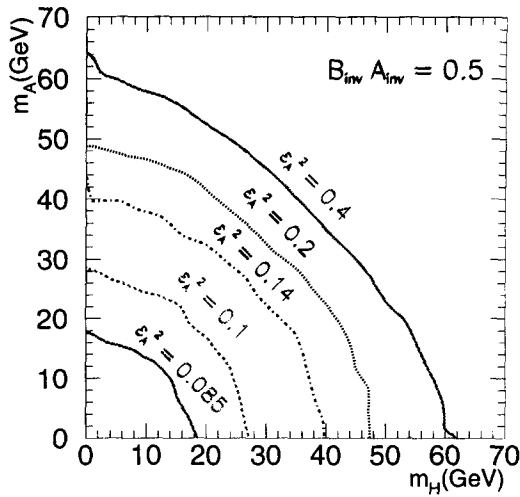


Fig. 6. 95% CL bounds on  $\epsilon_A^2$  in the  $m_{H_1}$ - $m_A$  plane for the indicated value of the invisible branching ratios

restrictions on the parameters of the Higgs potential of this model, especially because of its complexity. However, we analyze all signatures that can be engendered by Higgs boson production and its subsequent decays in this model. Although tedious, it is a straightforward task to convert the bare information we provide into restrictions on the model parameters. However, we prefer not perform this in detail and use the underlying model only to motivate the analysis.

First we study the constraints arising from the invisible  $Z$  width, following closely the analysis performed in Ref. [25], where a simpler model, with lepton number violation introduced explicitly and the Higgs bosons decaying to neutrinos rather than to majorons was analyzed. As in the case of the model in Ref. [25], the Bjorken process contribution to the invisible  $Z$  width  $Z \rightarrow Z^* H_1$  is very small. Therefore we consider the limits that can be set on associated Higgs boson production at the  $Z$  peak,  $e^+ e^- \rightarrow Z \rightarrow H_1 A$  when both  $CP$ -even ( $H_1$ ) as well as  $CP$ -odd Higgs bosons ( $A$ ) decay invisibly. The contribution to the invisible  $Z$  width in terms of invisible branching ratios  $B_{inv}$  and  $A_{inv}$  can be found in Ref. [25], and the invisible branching ratios themselves are defined in Eq. (37).

In Fig. 6 we show 95% CL bounds on  $\epsilon_A^2$  in the  $m_{H_1}$ - $m_A$  plane for a fixed illustrative value of the product  $B_{inv} A_{inv} = 0.5$ . Five curves labelled by a value of  $\epsilon_A^2$  are shown. No points below each of these curves are allowed with  $\epsilon_A^2$  larger than that value. The corresponding exclusion plot corresponding to  $B_{inv} A_{inv} = 1$  has been given in Ref. [25]. We see from these plots that simply by using the neutrino counting at the  $Z$  peak one can already impose important constraints on the parameters of the model. For example, for  $H_1$  and  $A$  masses around 20 GeV the upper bound on  $\epsilon_A^2$  is a few times  $10^{-2}$ .

Apart from an additional contribution to the invisible  $Z$  width, the model produces the variety of signals shown in Table 1. Most of these are exactly the same as analyzed in [14]. Though the analysis presented in Ref. [14] was in a different context, those

results are applicable here. They are summarized in Figs. 4 and 5 of Ref. [14]. These plots may be regarded as particular cases of our model when  $A_{\text{inv}} \rightarrow 0$ . With appropriate re-interpretation they can be adapted to our case. However, as we mentioned, we will not enter into that.

We now consider the various final state topologies that can be produced in  $e^+e^-$  collisions at LEP, for example those exhibiting  $b\bar{b}$  or  $\ell^+\ell^-$  ( $\ell = \mu$  or  $e$ ) pairs and missing energy. The complete table of signatures is reproduced in Table 1.

A lot of information follows from the detailed study of these signals. Of the topologies considered in Table 1, all have been previously analyzed in Ref. [14] by carefully evaluating the signals and backgrounds, and by choosing appropriate cuts to enhance the discovery limits. There is only one exception: the present model contains a completely novel signature, namely four b-jets plus missing momentum. This is not present in [14] nor in [25]. As far as we know it is the first extension of the Higgs sector with this feature. Therefore, from now on we concentrate on this  $b\bar{b}b\bar{b}\cancel{p}_T$  signal. The main background comes from  $e^+e^- \rightarrow Z\gamma Z\gamma$ ,  $e^+e^- \rightarrow WW$  and  $e^+e^- \rightarrow Z\gamma$ . This background has been analyzed in other contexts, such as chargino production at LEP II [26,27], where two charginos are produced decaying each one into a neutralino plus a  $W$  boson, where the neutralino is stable or decays invisibly. This also gives the 4 jets + missing momentum signature. With appropriate cuts in the  $\cancel{p}_T$ , number of jets and invariant mass distributions the background could be removed keeping high signal efficiencies. For our illustrative purposes, we imposed the following cuts in order to remove the background:

- (i) when dealing with hadronic events we only select those events with at least 12 charged particles in the final state.
- (ii) In to avoid high energy initial state radiation  $Z$  events we reject events with a photon with an energy of more than 35 GeV
- (iii) We only accept events with at least four jets.
- (iv) We reject an event if the sum of the energy of the two less energetic jets is less than 10 GeV, in order to remove events like  $e^+e^- \rightarrow q\bar{q}g$ , and  $e^+e^- \rightarrow (Z \rightarrow q\bar{q})(\gamma^* \rightarrow q\bar{q})$  characterized by two very energetic jets plus two less energetic ones.
- (v) We reject events with a missing transverse momentum smaller than 10 GeV, in order to avoid events with particles going down the beam pipe.
- (vi) We finally impose the invariant mass of the event to  $m_{\text{inv}} > 100$  GeV. This cut is essential to kill the  $Z$  background, which has a large cross section.

Applying all these cuts we eliminate the background, that has been simulated using JETSET [28]. We did a Monte Carlo study of the signal for our model, which allowed us to calculate the efficiency for the signature after implementing the above-mentioned cuts. Our results are given as a 95% CL exclusion plot in the  $M_H$ - $M_A$  plane shown in Fig. 7. We have assumed a LEP II integrated luminosity of  $300 \text{ pb}^{-1}$ . These results are complementary to those arising from the invisible width only, and also complement those that can be derived by appropriate rescaling of the plots shown in [14] corresponding to the other signals in Table 1.

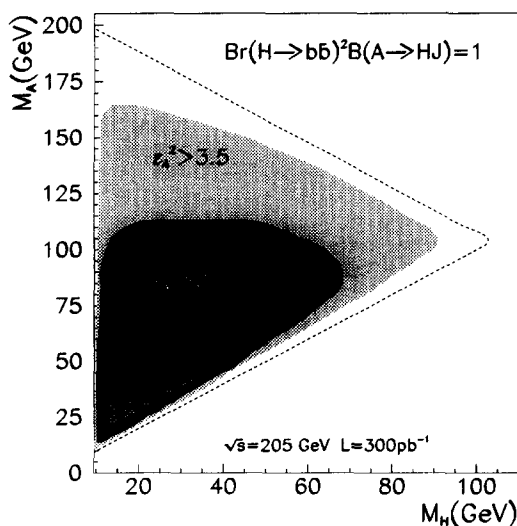


Fig. 7. 95% CL bounds on  $\epsilon_A^2$  in the  $m_H$ - $m_A$  plane that follow from the four-jets + missing transverse momentum analysis.

## 7. Conclusions

We have studied the neutral Higgs sector of the general seesaw majoron-type model of neutrino mass generation with spontaneous violation of lepton number. This sector contains three massive  $CP$ -even Higgs bosons  $H_i$ ,  $i = 1, 2, 3$ , one massive  $CP$ -odd  $A$ , and one massless  $CP$ -odd  $J$  called the majoron. We show that  $H_1$  and  $A$  can decay invisibly into majorons and determine the constraints that arise from the invisible decay width of the  $Z$  gauge boson. The existence of such novel invisible pseudoscalar Higgs boson decays discussed in this paper should be taken into account when determining the Higgs boson discovery prospects at LEP II and other colliders, such as the LHC and NLC.

We have also noted that the existence of the new decay channel  $A \rightarrow H_1 + J$  leads to a novel four-jet + missing momentum signature in associated Higgs boson production  $e^+e^- \rightarrow H_1 A$  when  $A \rightarrow H_1 J$  and  $H_1 \rightarrow b\bar{b}$ . This could be detectable at LEP II. We have studied the background and performed a Monte Carlo simulation of the signal in order to determine the limits that follow from that. Although the structure of the Higgs sector is quite rich one has already important restrictions on Higgs boson mass, couplings and branching ratios that should be taken into account in relation to possible new studies at future colliders such as the LHC [29] and the NLC [12] or at a possible muon collider.

## Acknowledgements

We thank A. Joshipura, J.J. Hernandez and S. Navas for useful discussions. Special thanks to Oscar Eboli for very helpful discussions related to the study presented in Section 6. This work was supported by DGICYT under grant PB95-1077 and by the TMR

network grant ERBFMRXCT960090 of the European Union. M.A.D. was supported by a DGICYT postdoctoral grant, D.A.R. was supported by Colombian COLCIENCIAS fellowship, while M.A.G.-J. was supported by a Spanish MEC FPI fellowship.

## References

- [1] P.W. Higgs, Phys. Lett. 12 (1964) 132;  
F. Englert and R. Brout, Phys. Rev. Lett. 13 (1964) 321;  
G. Guralnik and C.K. Hagen, Phys. Rev. Lett. 13 (1964) 585.
- [2] F. Richard, in Elementary Particle Physics: Present and Future, Proceedings of Valencia 95, ed. A. Ferrer and J.W.F. Valle, (World Scientific, Singapore, 1996) p. 3.
- [3] M. Carena and P. Zerwas et al., convenors, Higgs Physics, Proceedings of LEP2 Workshop, CERN Yellow Report, ed. G. Altarelli et al.
- [4] For a review see J.W.F. Valle, Prog. Part. Nucl. Phys. 26 (1991) 91 and references therein.
- [5] Y. Chikashige, R. Mohapatra and R. Peccei, Phys. Lett. B 98 (1980) 265.
- [6] J.E. Kim, Phys. Rep. 150 (1987) 1 and references therein.
- [7] A. Joshipura and J.W.F. Valle, Nucl. Phys. B 397 (1993) 105 and references therein.
- [8] A.S. Joshipura and S. Rindani, Phys. Rev. Lett. 69 (1992) 3269.
- [9] F. de Campos and J.W.F. Valle, Phys. Lett. B 292 (1992) 329;  
A. Masiero and J.W.F. Valle, Phys. Lett. B 251 (1990) 273;  
J.C. Romão, C.A. Santos and J.W.F. Valle, Phys. Lett. B 288 (1992) 311.
- [10] A. Lopez-Fernandez, J.C. Romão, F. de Campos and J.W.F. Valle, Phys. Lett. B 312 (1993) 240.
- [11] B. Brahmachari, A.S. Joshipura, S. Rindani, D.P. Roy and K. Sridhar, Phys. Rev. D 48 (1993) 4224.
- [12] O.J.P. Eboli, M.C. Gonzalez-Garcia, A. Lopez-Fernandez, S.F. Novaes, J.W.F. Valle, O.J.P. Éboli et al., Nucl. Phys. B421 (1994) 65 [hep-ph/9312278];  
F. de Campos et al., Working Group on  $e^+e^-$  Collision at 500 GeV: The Physics Potential, ed. P. Zerwas (1993) p. 55.
- [13] F. de Campos, M.A. Garcia-Jareño, A.S. Joshipura, J. Rosiek, D.P. Roy and J.W.F. Valle, Phys. Lett. B 336 (1994) 446.
- [14] F. de Campos, O.J.P. Eboli, J. Rosiek, J.W.F. Valle, Phys. Rev. D 55 (1997) 1316.
- [15] For a recent LEP analysis see M. Acciarri et al. (L3 Collaboration), CERN-PPE-97-097, July 1997, submitted to Phys. Lett. B.
- [16] M. Gell-Mann, P. Ramond and R. Slansky, in Supergravity, ed. D. Freedman et al. (North-Holland, Amsterdam, 1979);  
T. Yanagida, KEK lectures, ed. O. Sawada et al. (1979).
- [17] R. Mohapatra, G. Senjanovic, Phys. Rev. D 23 (1981) 165.
- [18] J. Schechter and J.W.F. Valle, Phys. Rev. D 22 (1980) 2227.
- [19] J. Schechter and J.W.F. Valle, Phys. Rev. D 25 (1982) 774.
- [20] G.B. Gelmini and M. Roncadelli, Phys. Lett. B 99 (1981) 411.
- [21] H.M. Georgi, S.L. Glashow and S. Nussinov, Nucl. Phys. B 193 (1981) 297.
- [22] A.S. Joshipura, Int. J. Mod. Phys. A 7 (1992) 2021.
- [23] A. Pich, in Physics Beyond the Standard Model: Present and Future, Proceedings of Valencia 97, ed. I. Antoniadis, L.E. Ibáñez and J.W.F. Valle, to be published.
- [24] A. Djouadi, J. Kalinowski and P.M. Zerwas, Z. Phys. C57 (1993), 569 (1992).
- [25] M.A. Díaz, M.A. Garcia-Jareño, D.A. Restrepo and J.W.F. Valle, hep-ph/9712487, Dec. 1997 (to appear in Phys. Rev. D).
- [26] DELPHI Coll., P. Abreu et al., Europhys. J. C 1 (1998) 1.
- [27] F. de Campos, O.J.P. Eboli, M.A. García-Jareño and J.W.F. Valle, hep-ph/9710545 (submitted to Nucl. Phys. B).
- [28] T. Sjöstrand, Comp. Phys. Comm. 39(1986)347; PYTHIA 5.6 and JETSET 7.3, CERN-TH/6488-92.
- [29] J. Guion, Phys. Rev. Lett. 72 (1994) 199;  
D. Choudhury and D.P. Roy, Phys. Lett. B322 (1994) 368;  
J.C. Romão, F. de Campos, L. Diaz-Cruz and J.W.F. Valle, Mod. Phys. Lett. A9 (1994) 817;  
S.G. Frederiksen, N.P. Johnson, G.L. Kane and J.H. Reid, Phys. Lett. D50 (1994) 4244.